STIX challenges

Università di Genova
DIMA | Dipartimento di Matematica

Anna Volpara

Dolomites Research Week on Approximation and Applications
September, 2023

Outline

1. Calibration
2. New imaging method
3. Electron visibilities

STIX - Spectrometer/Telescope for Imaging X-rays

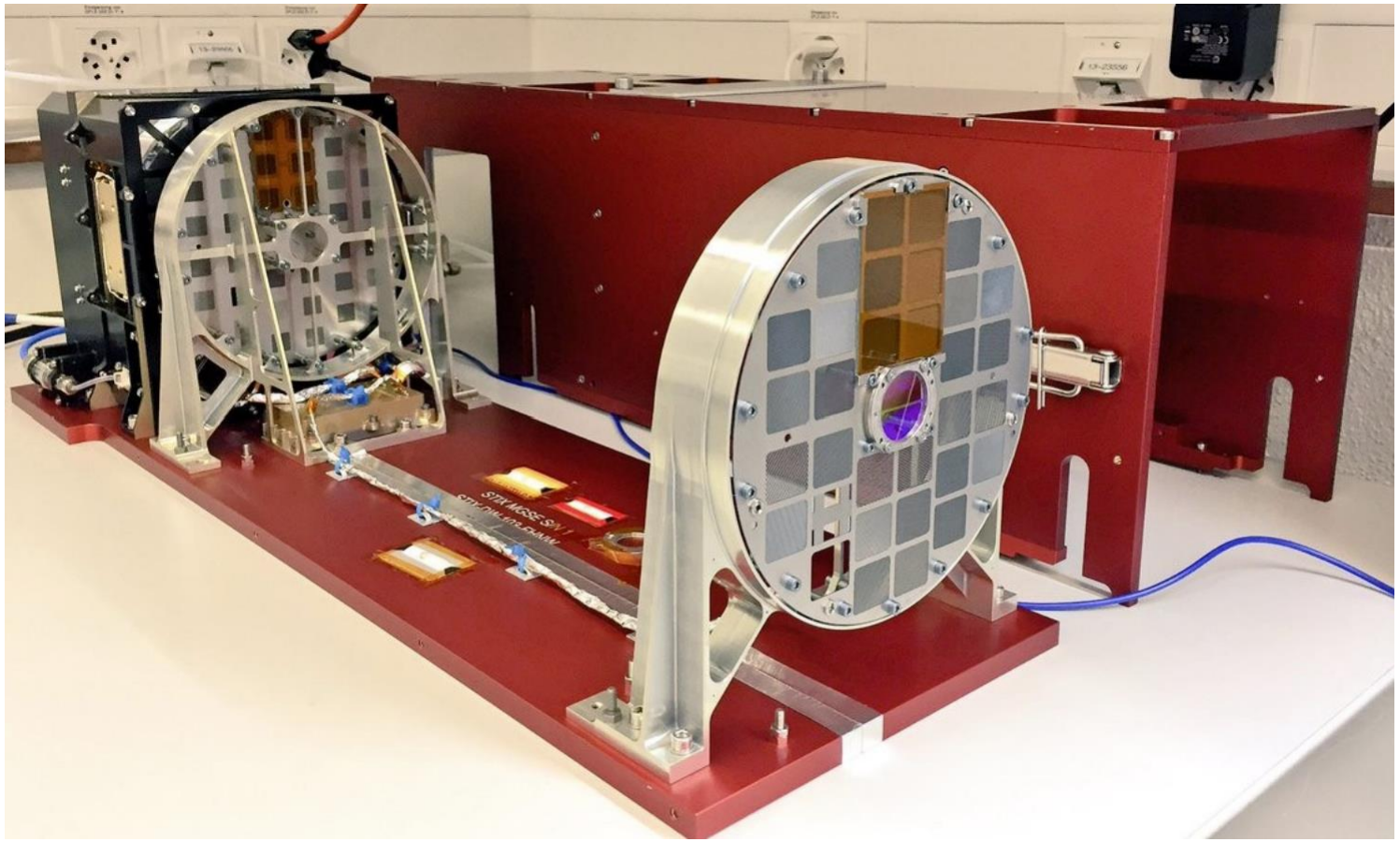

Figure: STIX before being assembled on Solar Orbiter (Krucker et al., 2020).

Massa P., et al. *STIX imaging I--Concept*. *arXiv preprint arXiv*, 2023.

STIX - Spectrometer/Telescope for Imaging X-rays

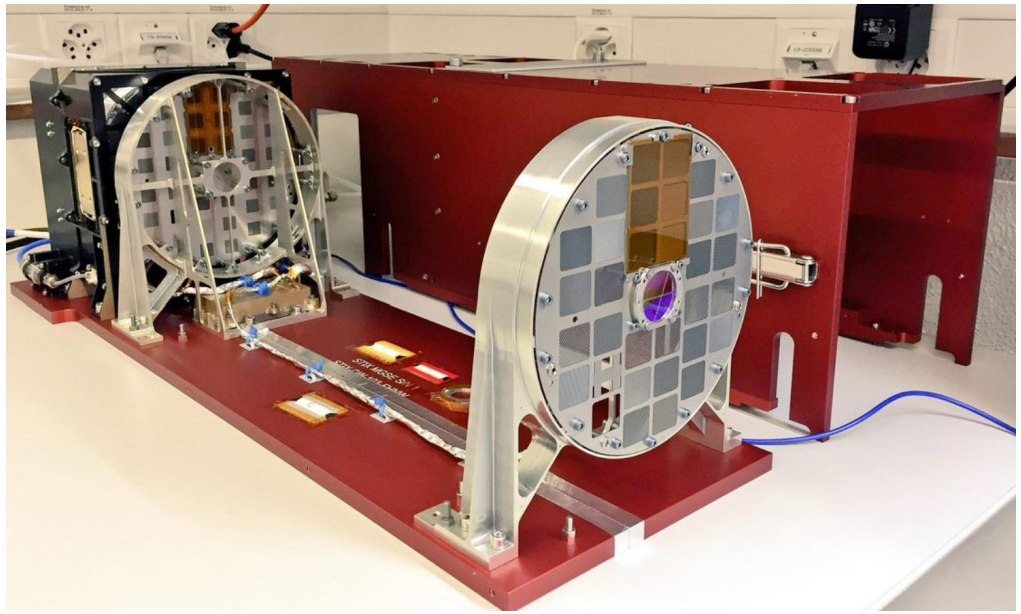

Figure: STIX before being assembled on Solar Orbiter (Krucker et al., 2020).

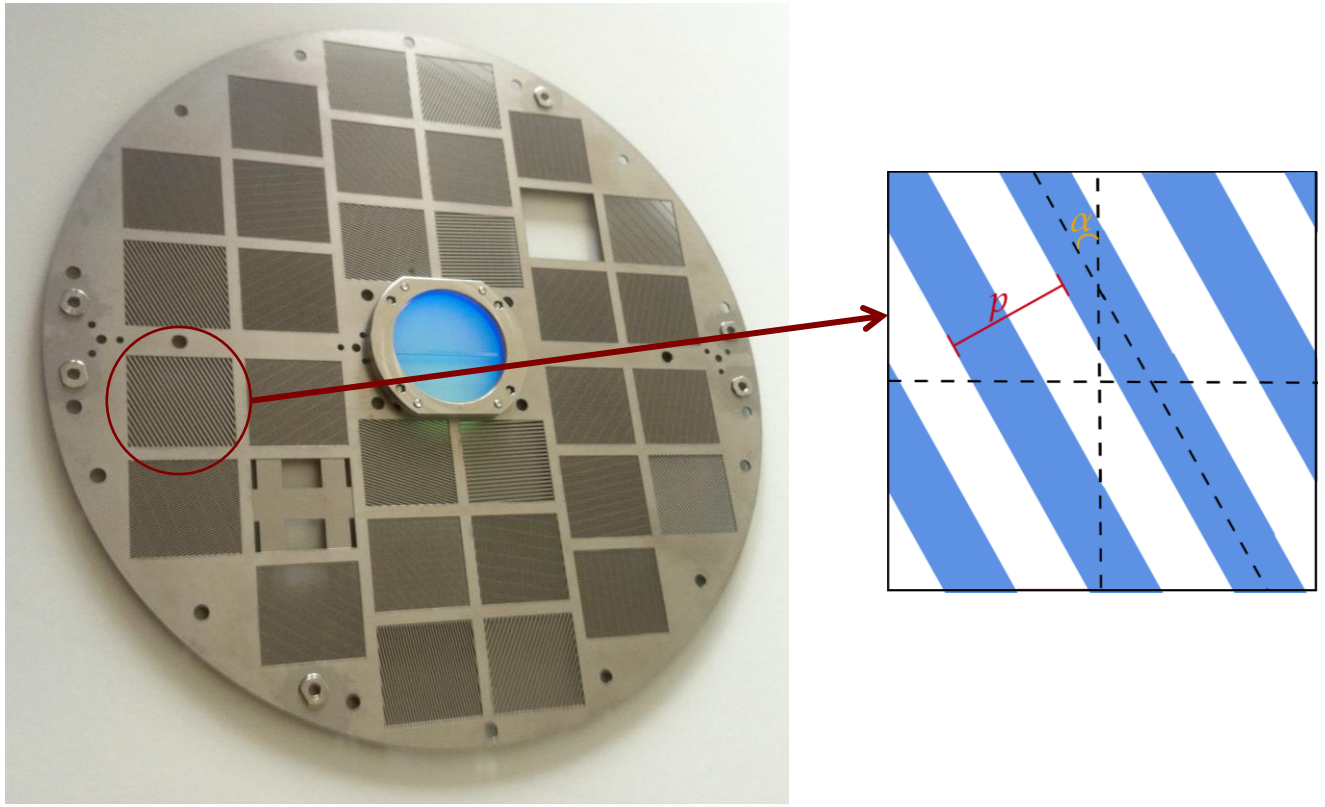

Figure: front and the rear grids before being assembled on the spacecraft (*left panel*), schematic of a grid window (*right panel*).

Massa P., et al. *STIX imaging I--Concept*. *arXiv preprint arXiv*, 2023.

STIX - Spectrometer/Telescope for Imaging X-rays

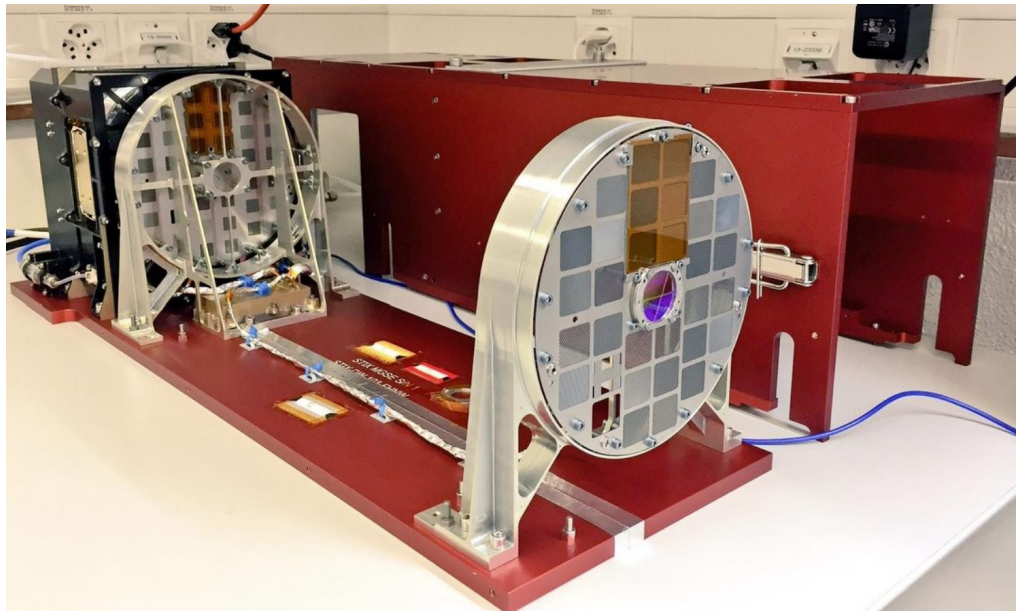

Figure: STIX before being assembled on Solar Orbiter (Krucker et al., 2020).

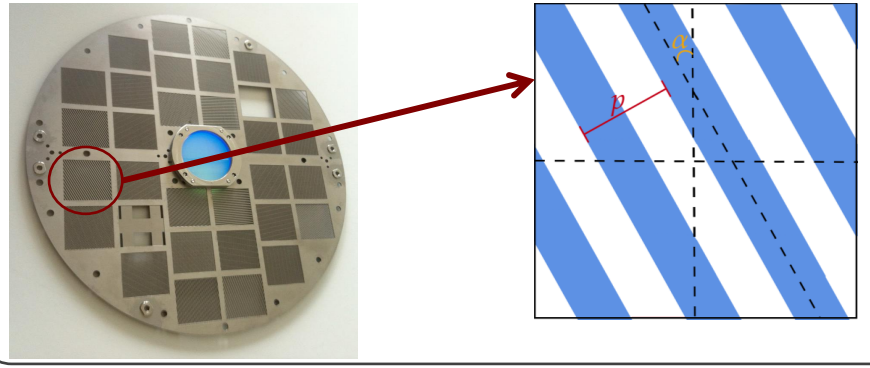

Figure: front and the rear grids before being assembled on the spacecraft (*left panel*), schematic of a grid window (*right panel*).

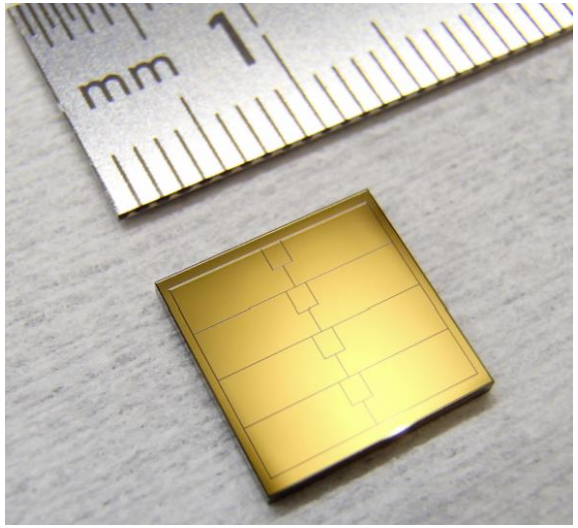

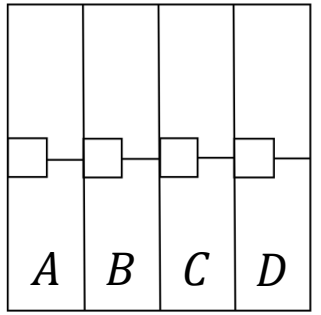

Figure: STIX detector (*left panel*) schematic of a detector (*right panel*).

Massa P., et al. *STIX imaging I--Concept*. *arXiv preprint arXiv*, 2023.

STIX - Spectrometer/Telescope for Imaging X-rays

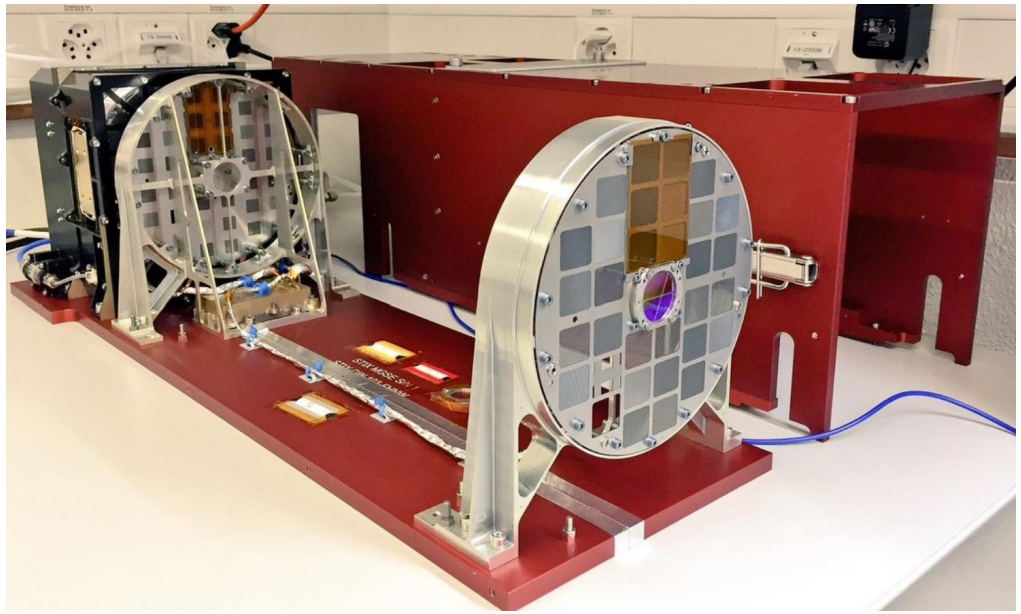

Figure: STIX before being assembled on Solar Orbiter (Krucker et al., 2020).

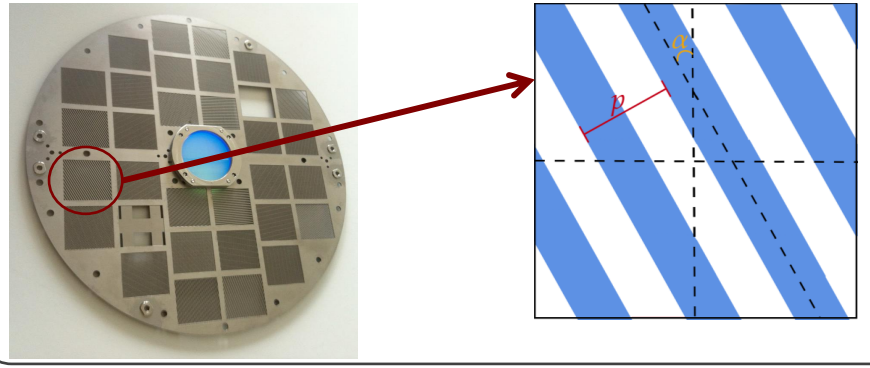

Figure: front and the rear grids before being assembled on the spacecraft (*left panel*), schematic of a grid window (*right panel*).

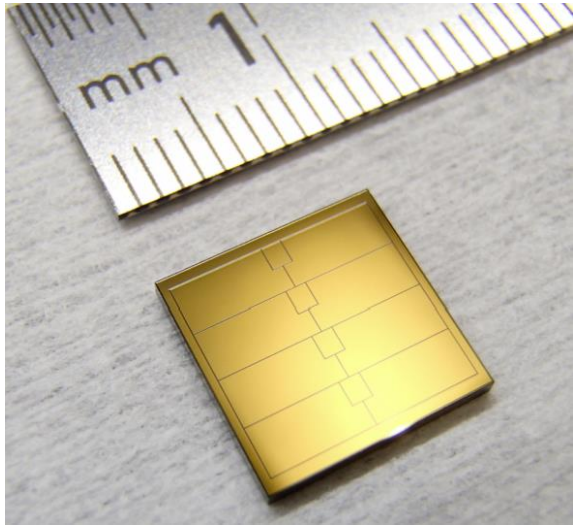

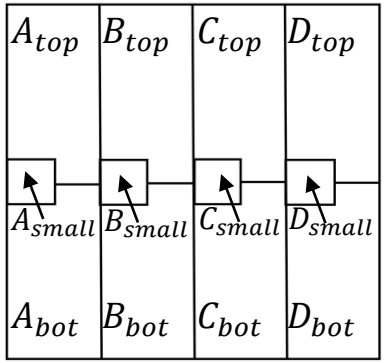

Figure: STIX detector (*left panel*) schematic of a detector (*right panel*).

Massa P., et al. *STIX imaging I--Concept*. *arXiv preprint arXiv*, 2023.

STIX - Spectrometer/Telescope for Imaging X-rays

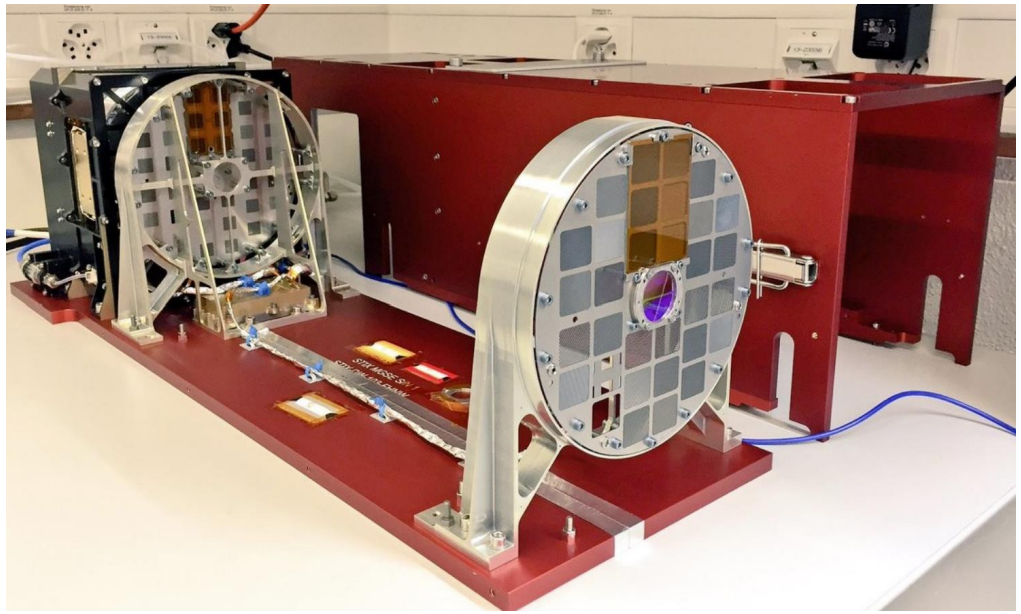

Figure: STIX before being assembled on Solar Orbiter (Krucker et al., 2020).

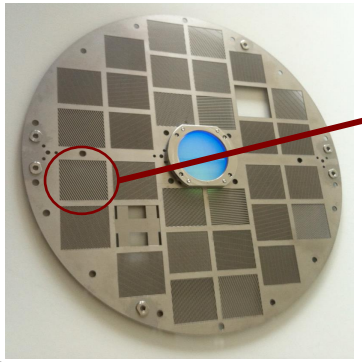

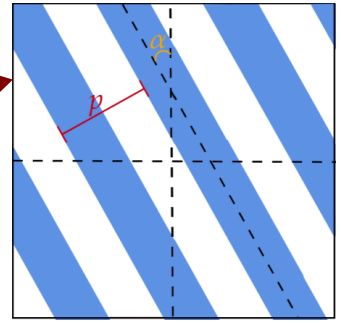

Figure: front and the rear grids before being assembled on the spacecraft (*left panel*), schematic of a grid window (*right panel*).

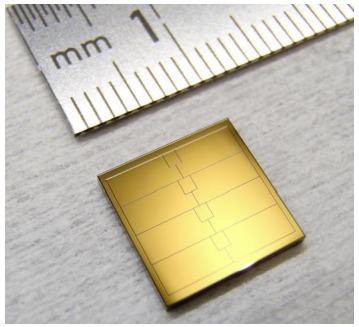

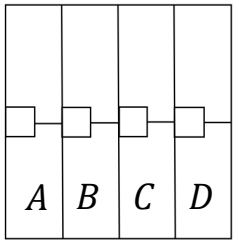

Figure: STIX detector (*left panel*) schematic of a detector (*right panel*).

Front grid + *Rear grid* + *detector* } Sub-collimator

Massa P., et al. *STIX imaging I--Concept*. *arXiv preprint arXiv*, 2023.

STIX data formation process

Image reconstruction problem for STIX:

$$\mathcal{F}\phi = \mathsf{V} \tag{1}$$

Massa P., et al. *STIX imaging I--Concept*. *arXiv preprint arXiv*, 2023.

STIX data formation process

Image reconstruction problem for STIX:

$$\mathcal{F}\phi = \mathrm{V} \qquad (1)$$

Intensity of the X-ray photon flux emitted from (x, y) on the Sun

Massa P., et al. *STIX imaging I--Concept*. *arXiv preprint arXiv*, 2023.

STIX data formation process

Image reconstruction problem for STIX:

$$\mathcal{F}\phi = \mathrm{V} \qquad (1)$$

Array containing the N_V complex values of the visibilities measured by STIX

$$|V| \propto \sqrt{(C-A)^2 + (D-B)^2}$$

$$\psi = \mathrm{atan}\left(\frac{D-B}{C-A}\right) + 45° + \psi_{\mathrm{calib}}$$

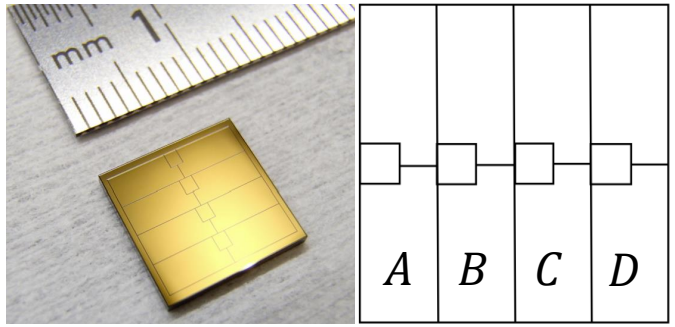

Figure: STIX detector (*left panel*) schematic of a detector (*right panel*).

Massa P., et al. *STIX imaging I--Concept*. *arXiv preprint arXiv*, 2023.

STIX data formation process

Image reconstruction problem for STIX:

$$\mathcal{F}\phi = \mathsf{V} \qquad (1)$$

The Fourier Transform defined by:

$$(\mathcal{F}\phi)_k = \iint \phi(x,y)\exp\left(2\pi i(xu_k + yv_k)\right)\,dx\,dy \quad k = 1,\ldots,N_v$$

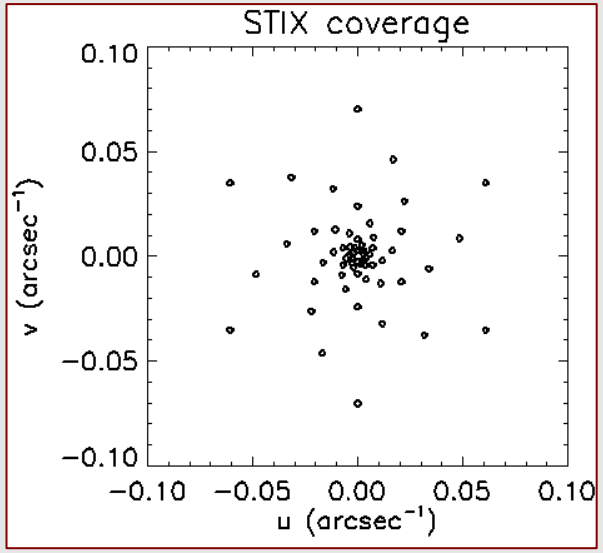

Figure: (u, v) frequencies sampled by STIX sub-collimators.

Massa P., et al. *STIX imaging I--Concept*. *arXiv preprint arXiv*, 2023.

Outline

1. **Calibration**
2. New imaging method
3. Electron visibilities

Two layers grid parameters

GOAL: Derive the parameters of the double (and triple) layers grids in order to treat them as single-layer grids.

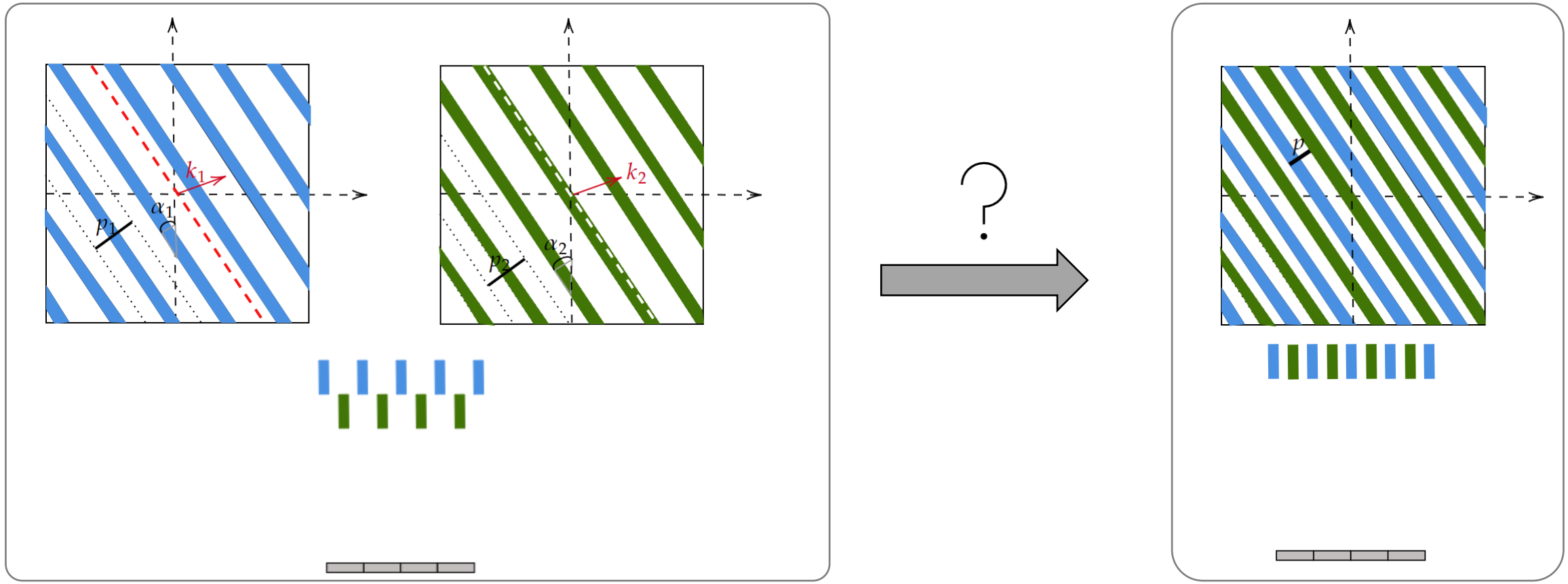

Test imaging – August 26, 2021

Time Interval: 23:18:00 – 23:20:00 UT
Energy Range: 15 – 25 keV

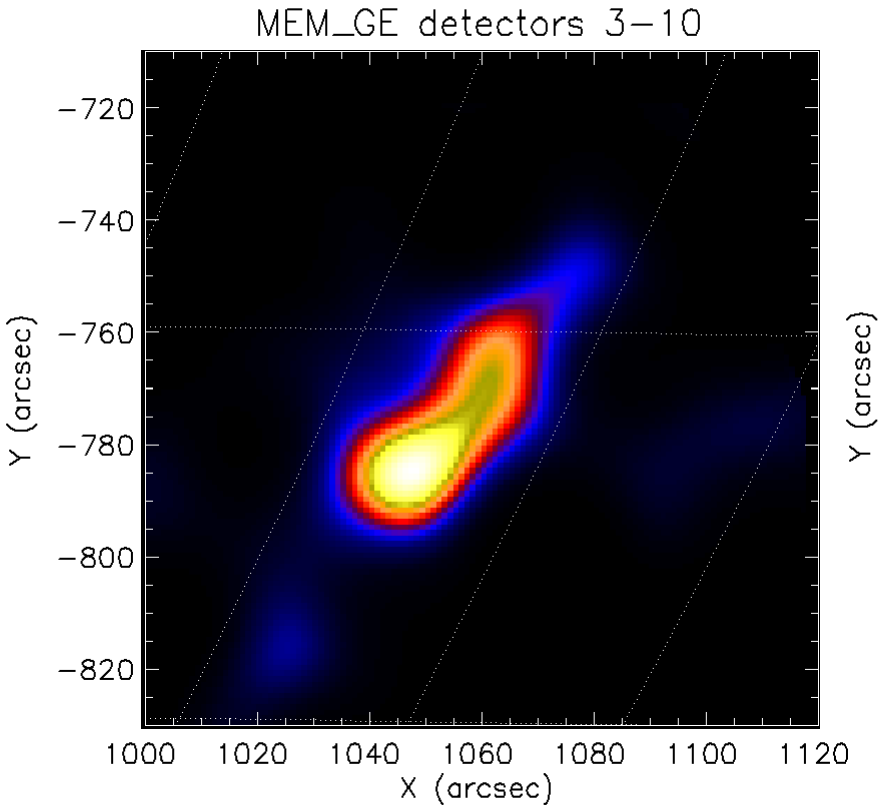

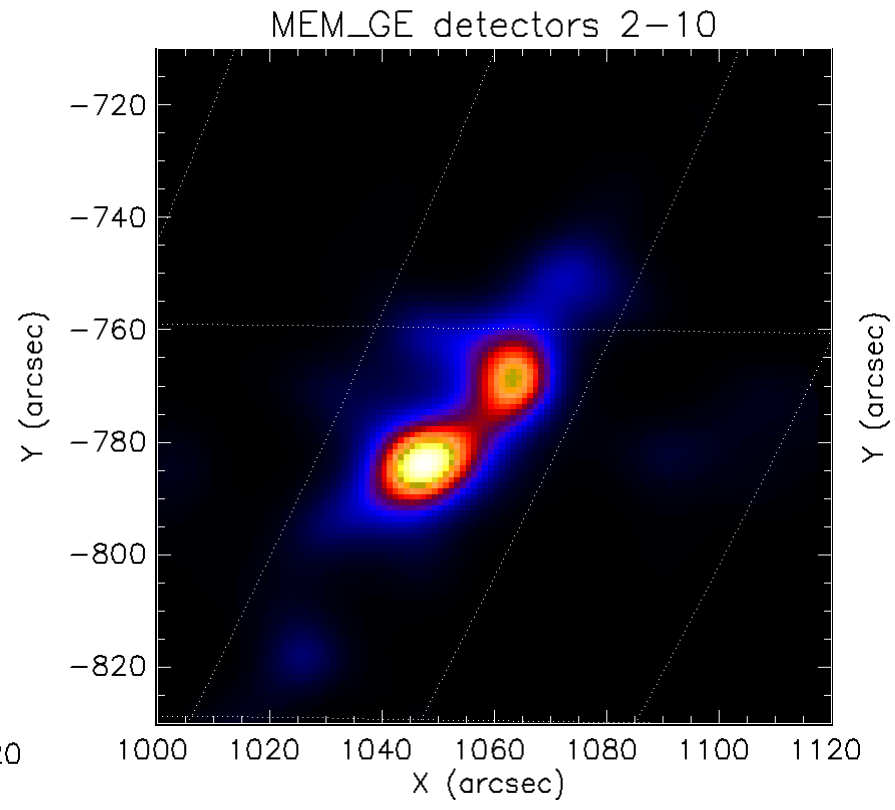

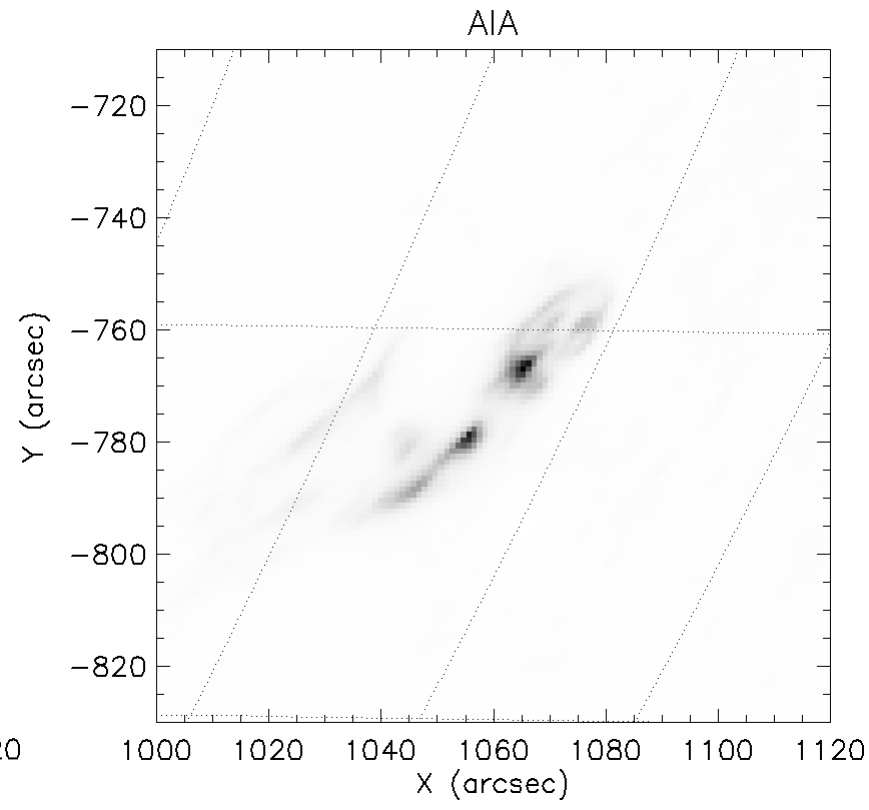

Test imaging – January 6, 2023

Time_range = 00:55:00 – 00:57:00 UT

Energy Range = 22 – 28 keV

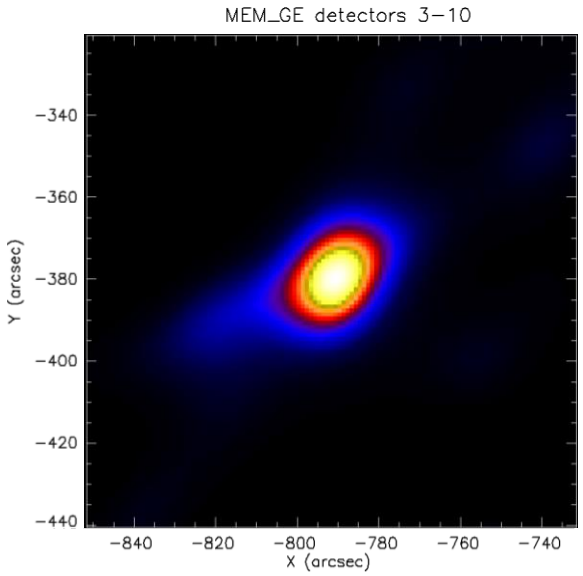

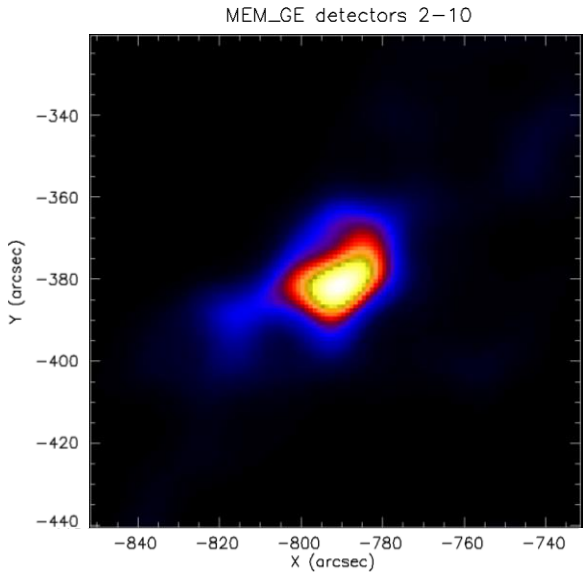

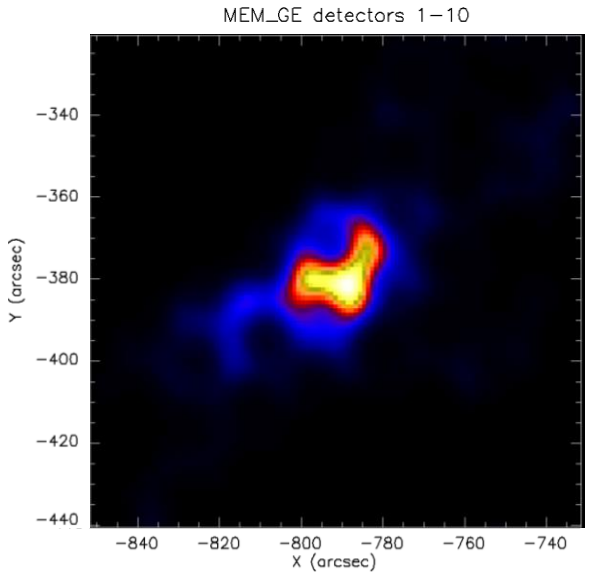

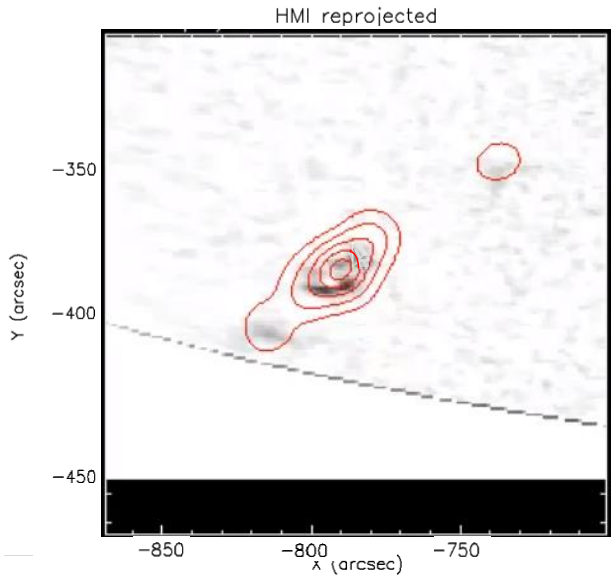

Total flux – Measured slit

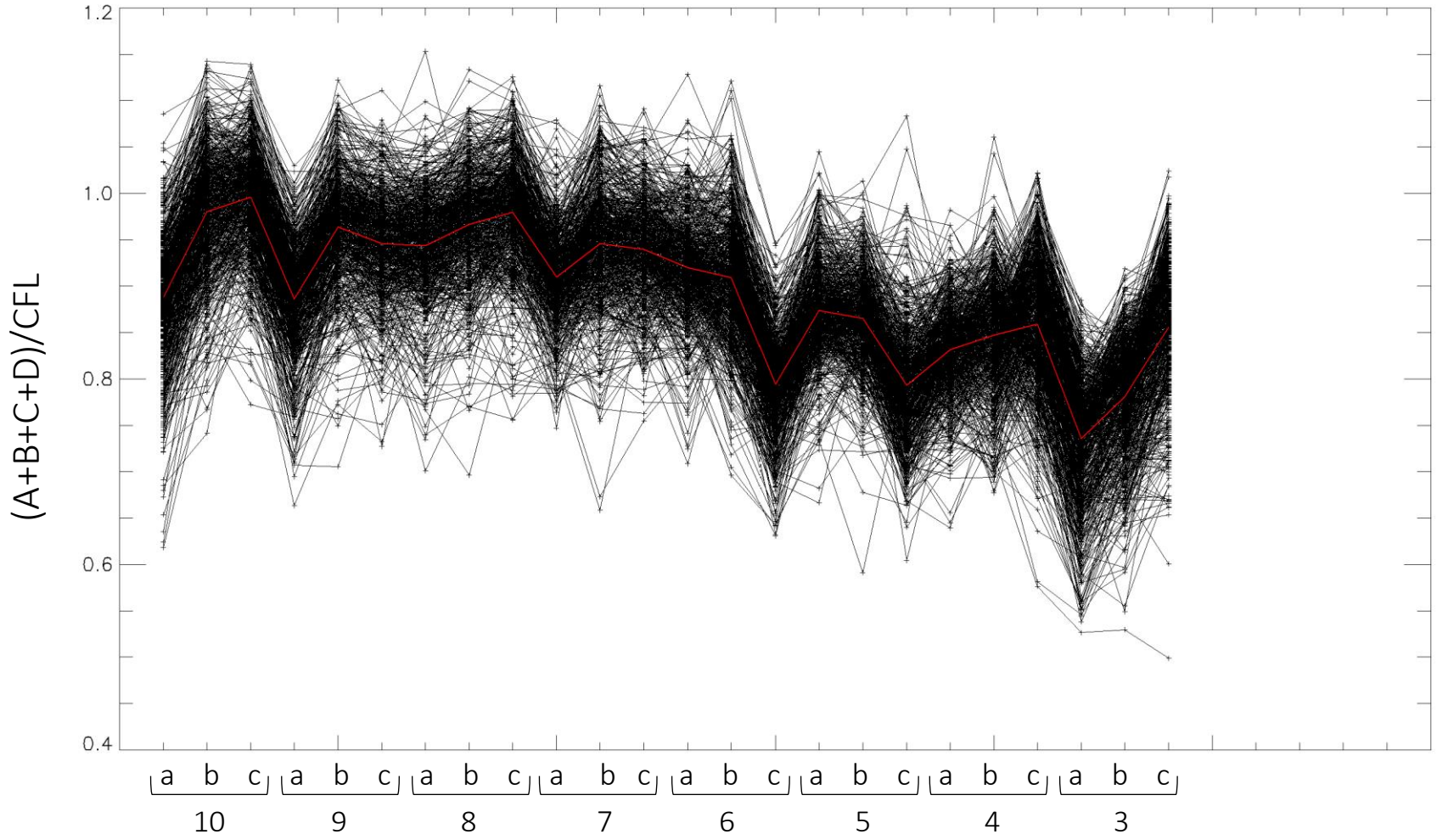

Figure: ratio between the total flux recorded by detectors from 3 to 10 and the flux recorded by CFL, for 700 events.

Total flux – Measured slit

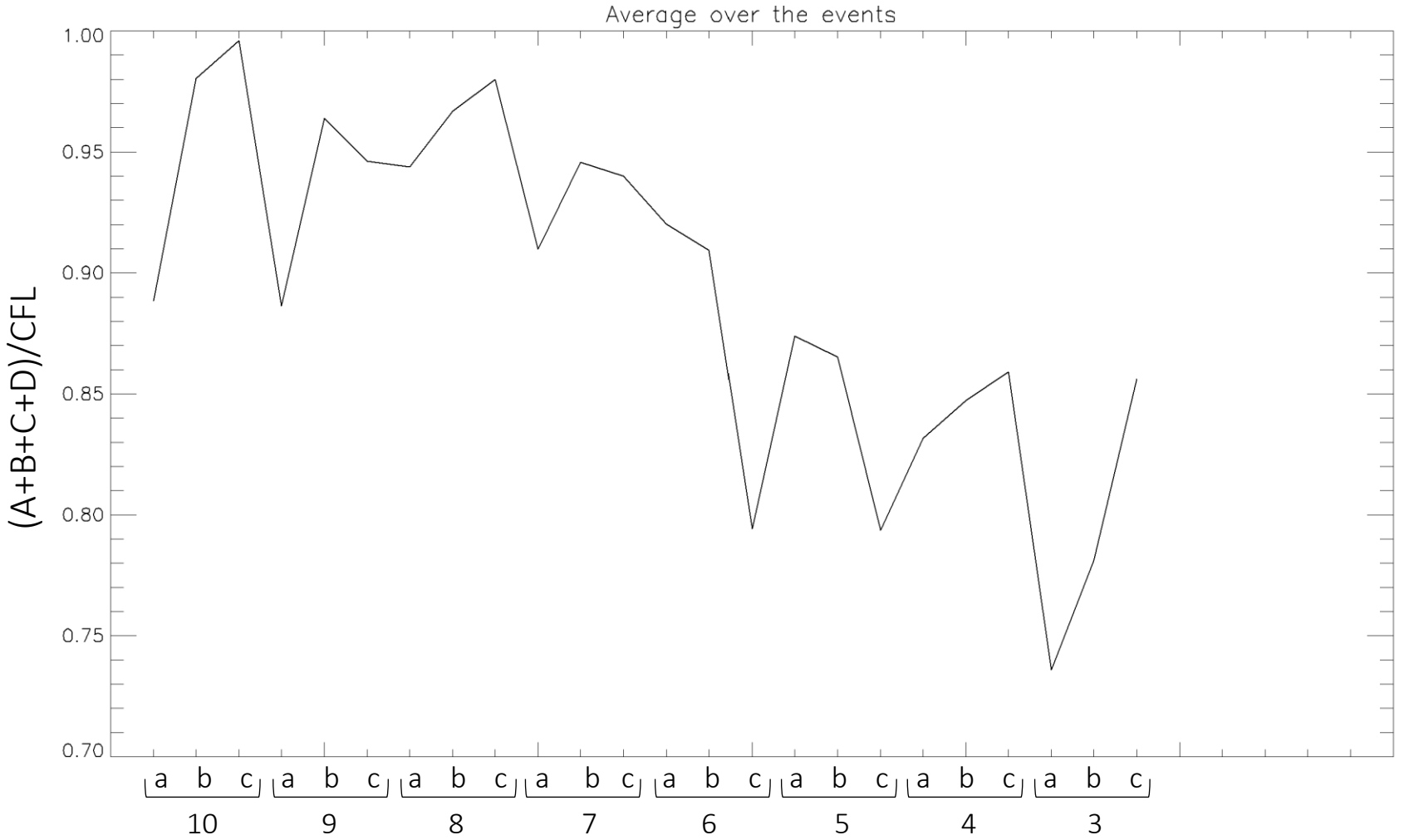

Figure: average of the ratio between the total flux recorded by detectors from 3 to 10 and the flux recorded by CFL, for 700 events.

Total flux – Measured slit

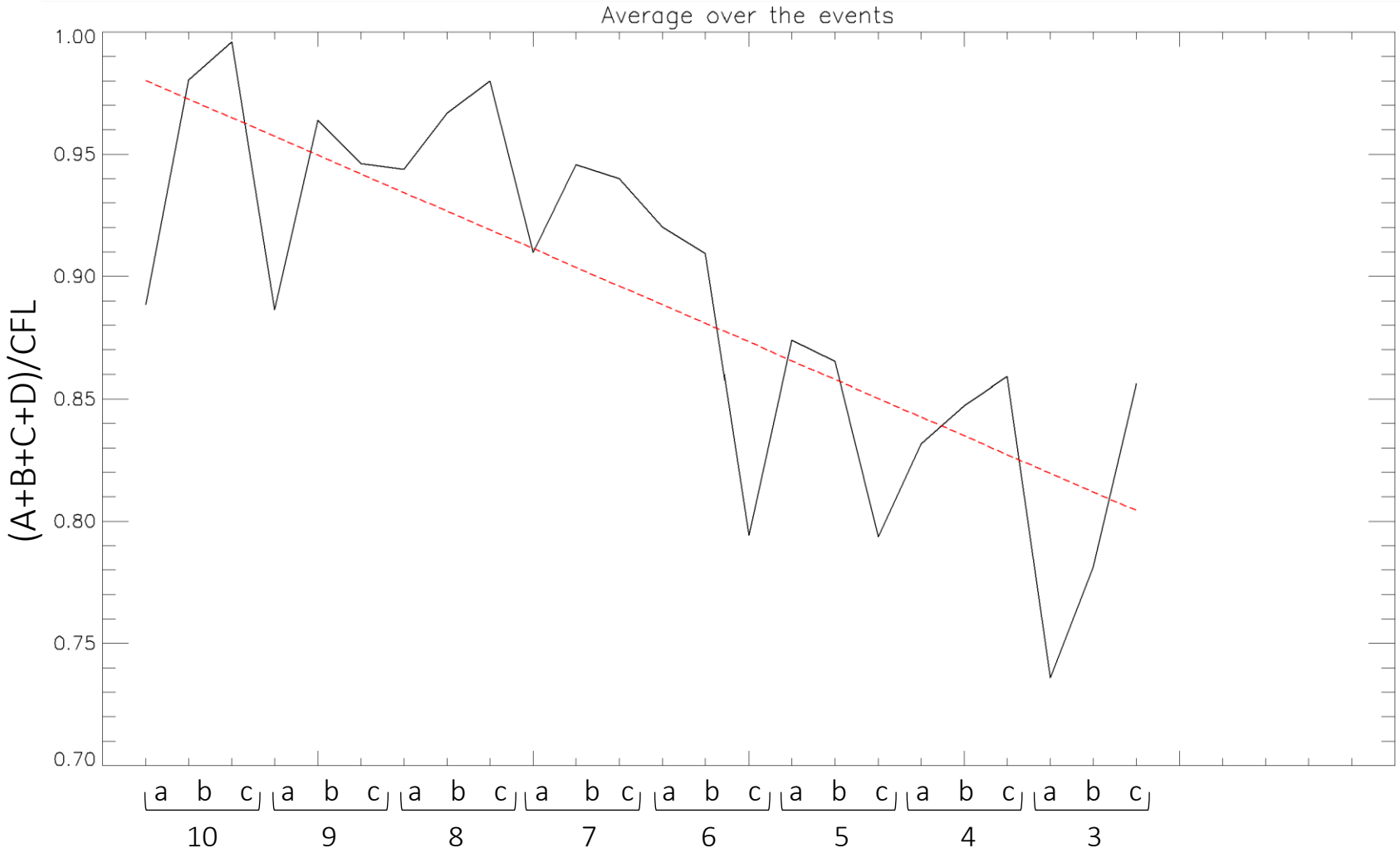

Figure: average of the ratio between the total flux recorded by detectors from 3 to 10 and the flux recorded by CFL, for 700 events.

Total flux – Effective slit

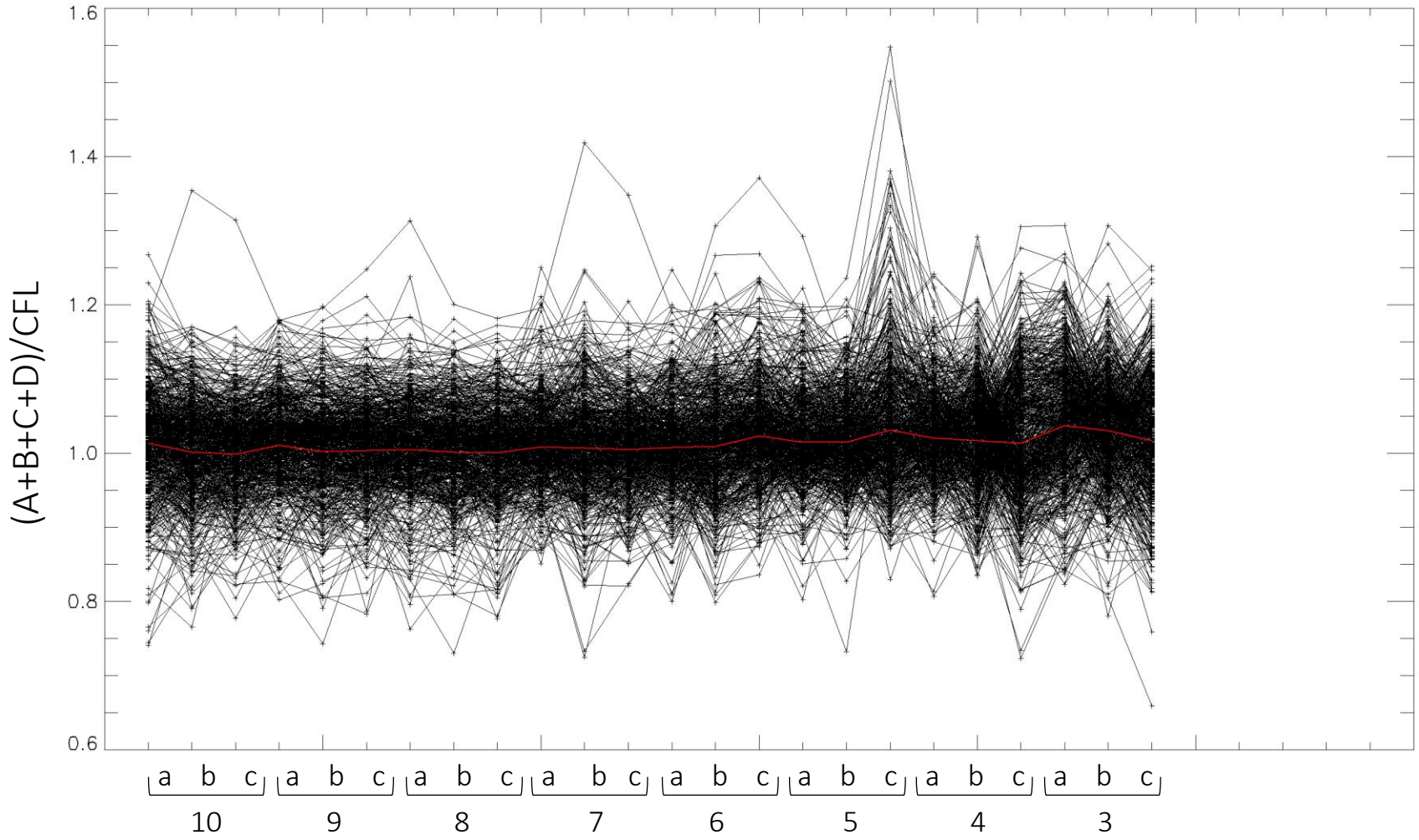

Figure: ratio between the total flux recorded by detectors from 3 to 10 and the flux recorded by CFL.

Outline

1. Calibration
2. **New imaging method**
3. Electron visibilities

MULTISCALE CLEAN

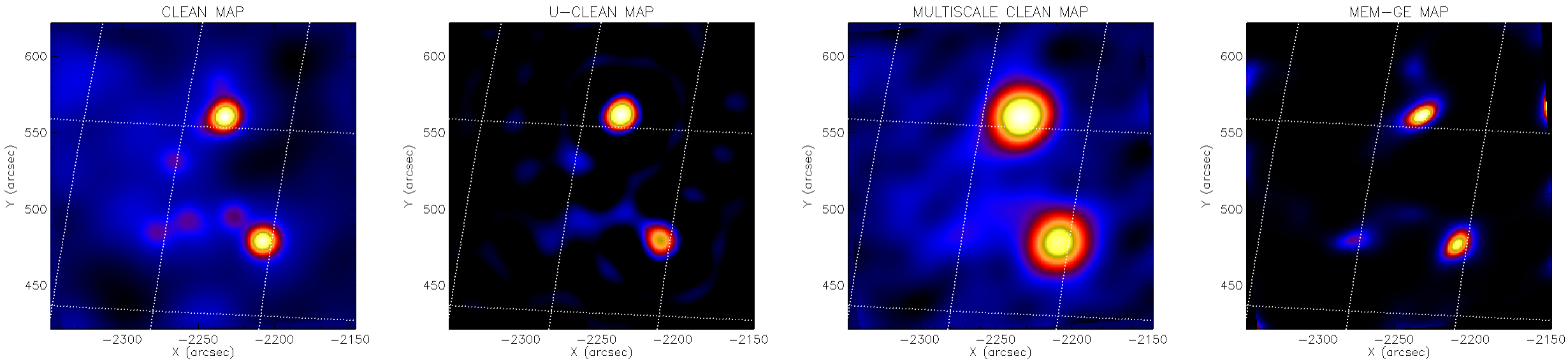

Figure: March 31, 2022 event; energy range: 25 – 50 keV. From left to right, reconstruction provided by CLEAN, U-CLEAN, MULTISCALE CLEAN and MEM_GE, respectively.

	CLEAN	U-CLEAN	MULTISCALE CLEAN	MEM-GE
Time elapsed (s)	44.066	14.904	10.482	27.454
χ^2	23.73	7.24	6.14	4.21

MULTISCALE CLEAN

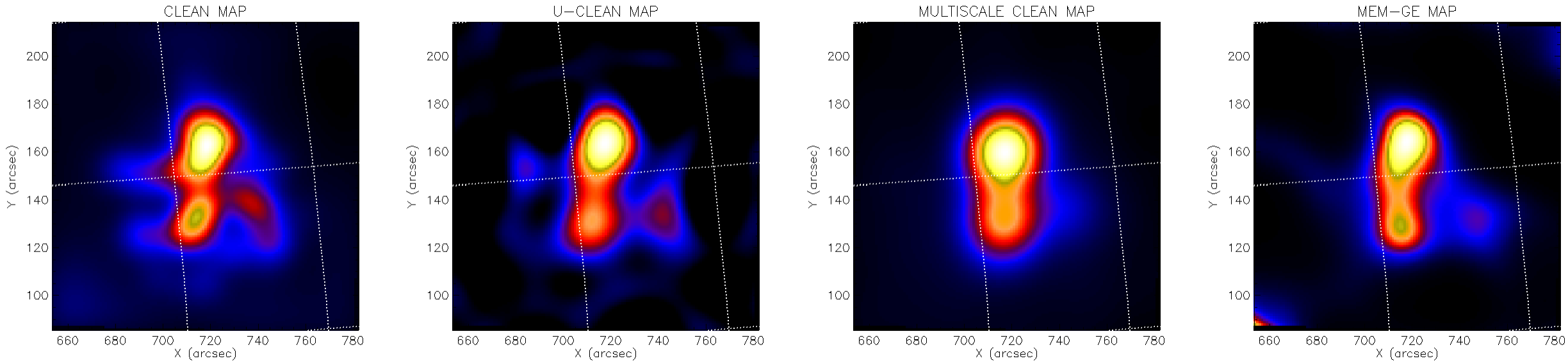

Figure: November 11, 2022 event; energy range: 6 – 10 keV. From left to right, reconstruction provided by CLEAN, U-CLEAN, MULTISCALE CLEAN and MEM_GE, respectively.

	CLEAN	U-CLEAN	MULTISCALE CLEAN	MEM-GE
Time elapsed (s)	38.440	4.799	18.672	6.342
χ^2	6.94	2.14	5.45	1.39

Outline

1. Calibration
2. New imaging method
3. **Electron visibilities**

From photon to electron visibilities

Bremsstralhung equation for visibilities:

$$V(u,v;\epsilon) = \int_{\epsilon}^{\infty} W(u,v;E)Q(\epsilon,E)\,dE \tag{2}$$

From photon to electron visibilities

Bremsstralhung equation for visibilities:

$$V(u,v;\epsilon) = \int_{\epsilon}^{\infty} W(u,v;E)Q(\epsilon,E)\,dE \tag{2}$$

Photon visibilities

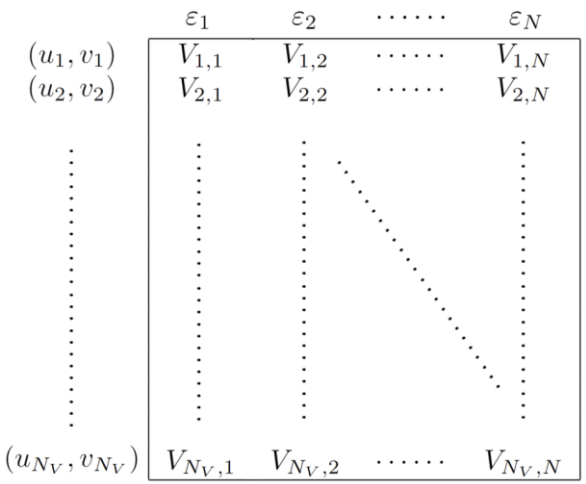

From photon to electron visibilities

Bremsstralhung equation for visibilities:

$$V(u,v;\epsilon) = \int_{\epsilon}^{\infty} W(u,v;E)Q(\epsilon,E)\,dE \qquad (2)$$

Spectral inversion via regularized inversion technique (Tikhonov)

Photon visibilities

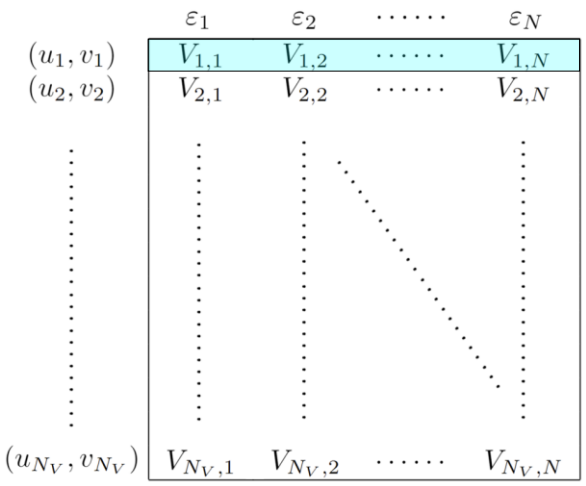

Electron visibilities

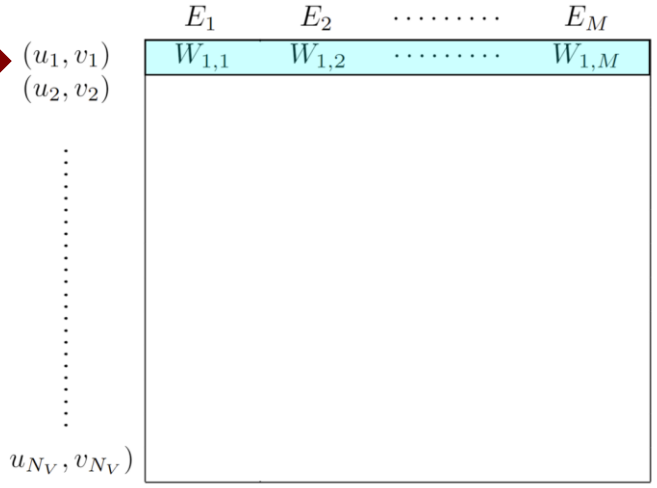

From photon to electron visibilities

Bremsstralhung equation for visibilities:

$$V(u,v;\epsilon) = \int_{\epsilon}^{\infty} W(u,v;E)Q(\epsilon,E)\,dE \qquad (2)$$

Spectral inversion via regularized inversion technique (Tikhonov)

Photon visibilities

$$\begin{array}{c|cccc} & \varepsilon_1 & \varepsilon_2 & \cdots\cdots & \varepsilon_N \\ (u_1,v_1) & V_{1,1} & V_{1,2} & \cdots\cdots & V_{1,N} \\ (u_2,v_2) & V_{2,1} & V_{2,2} & \cdots\cdots & V_{2,N} \\ \vdots & \vdots & \vdots & \ddots & \vdots \\ (u_{N_V},v_{N_V}) & V_{N_V,1} & V_{N_V,2} & \cdots\cdots & V_{N_V,N} \end{array}$$

Electron visibilities

$$\begin{array}{c|cccc} & E_1 & E_2 & \cdots\cdots\cdots & E_M \\ (u_1,v_1) & W_{1,1} & W_{1,2} & \cdots\cdots\cdots & W_{1,M} \\ (u_2,v_2) & W_{2,1} & W_{2,2} & \cdots\cdots\cdots & W_{2,M} \\ \vdots & \vdots & \vdots & \ddots & \vdots \\ (u_{N_V},v_{N_V}) & W_{N_V,1} & W_{N_V,2} & \cdots\cdots\cdots & W_{N_V,M} \end{array}$$

Products

Photon images

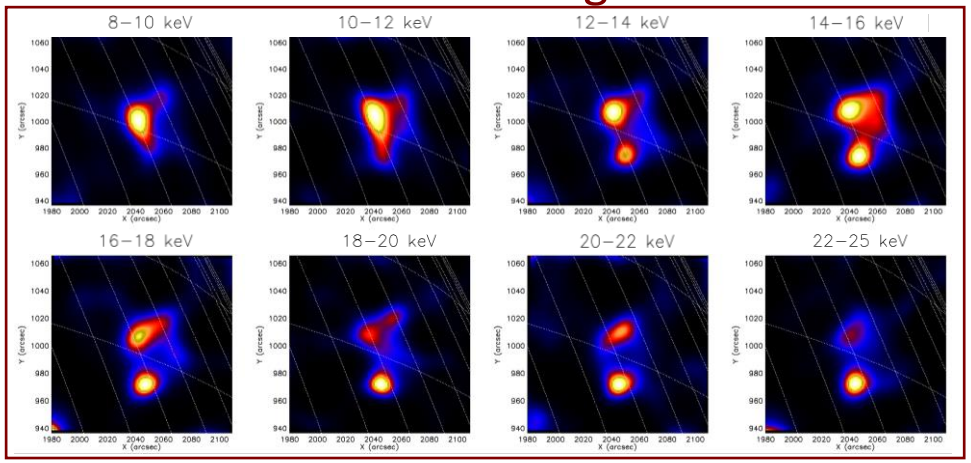

Regularized Photon images

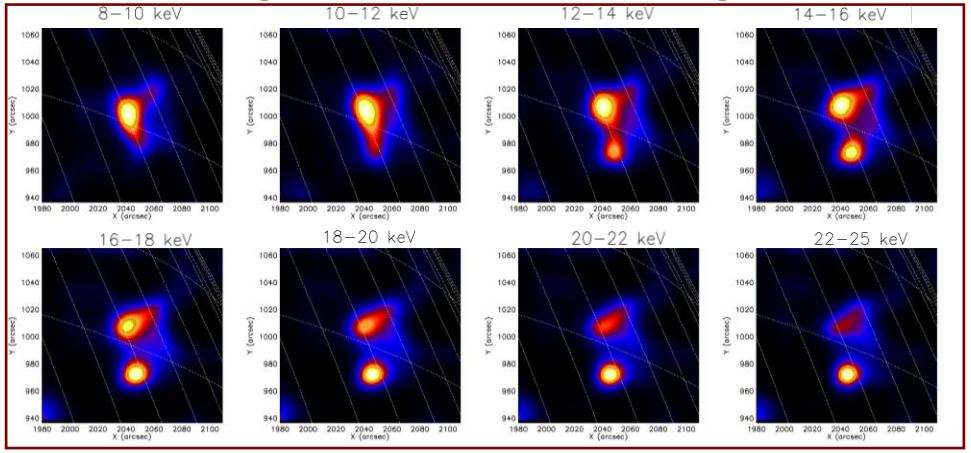

Electron flux images

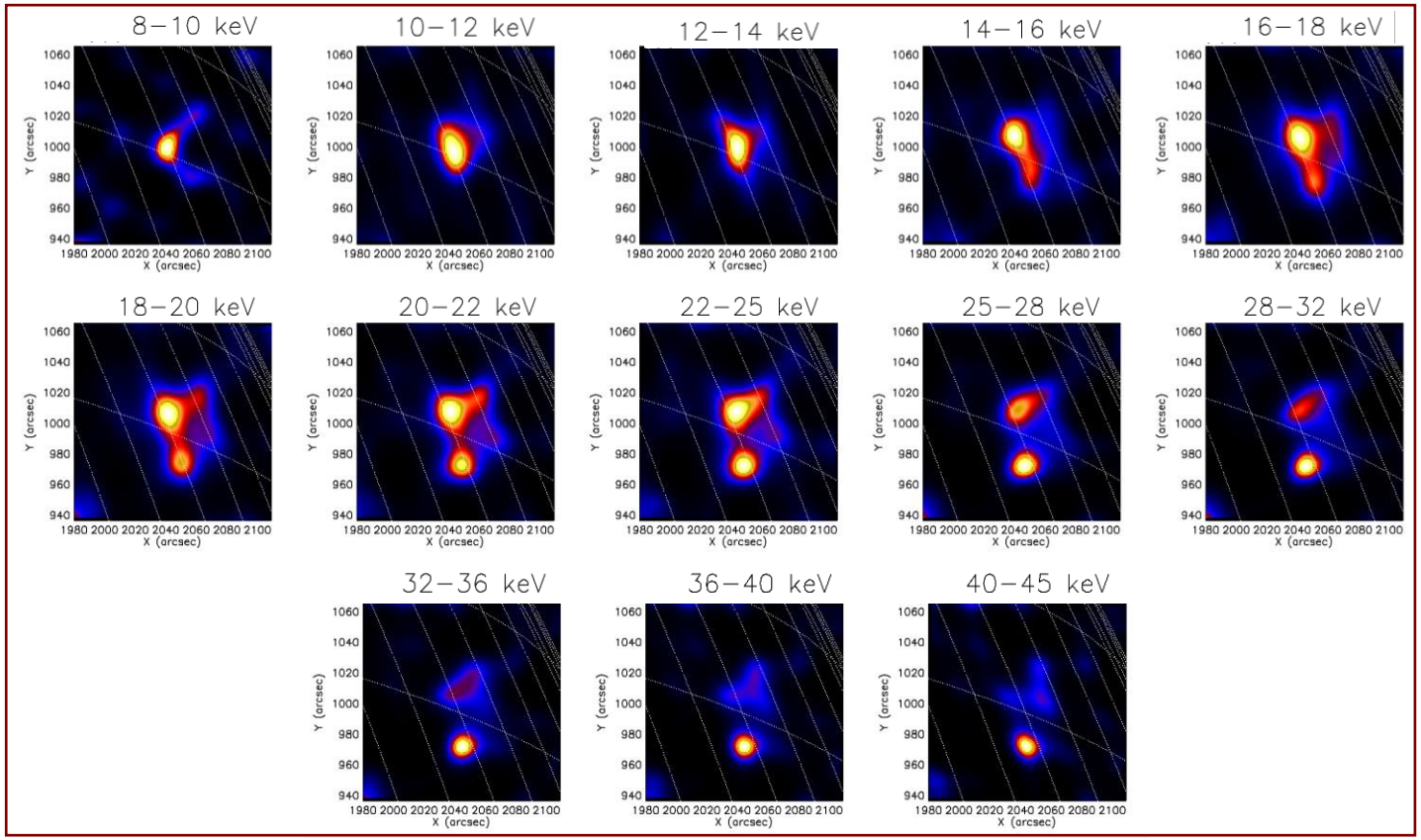

Figure: September 29, 2022 event. Photon images (*top left panels*) compared with the regularized photon maps (*bottom left panels*) in the same energy intervals, and electron flux images corresponding to the regularized electron visibilities (*right panels*) for the energy intervals shown. The maps are produced using the MEM-GE algorithm.

Products

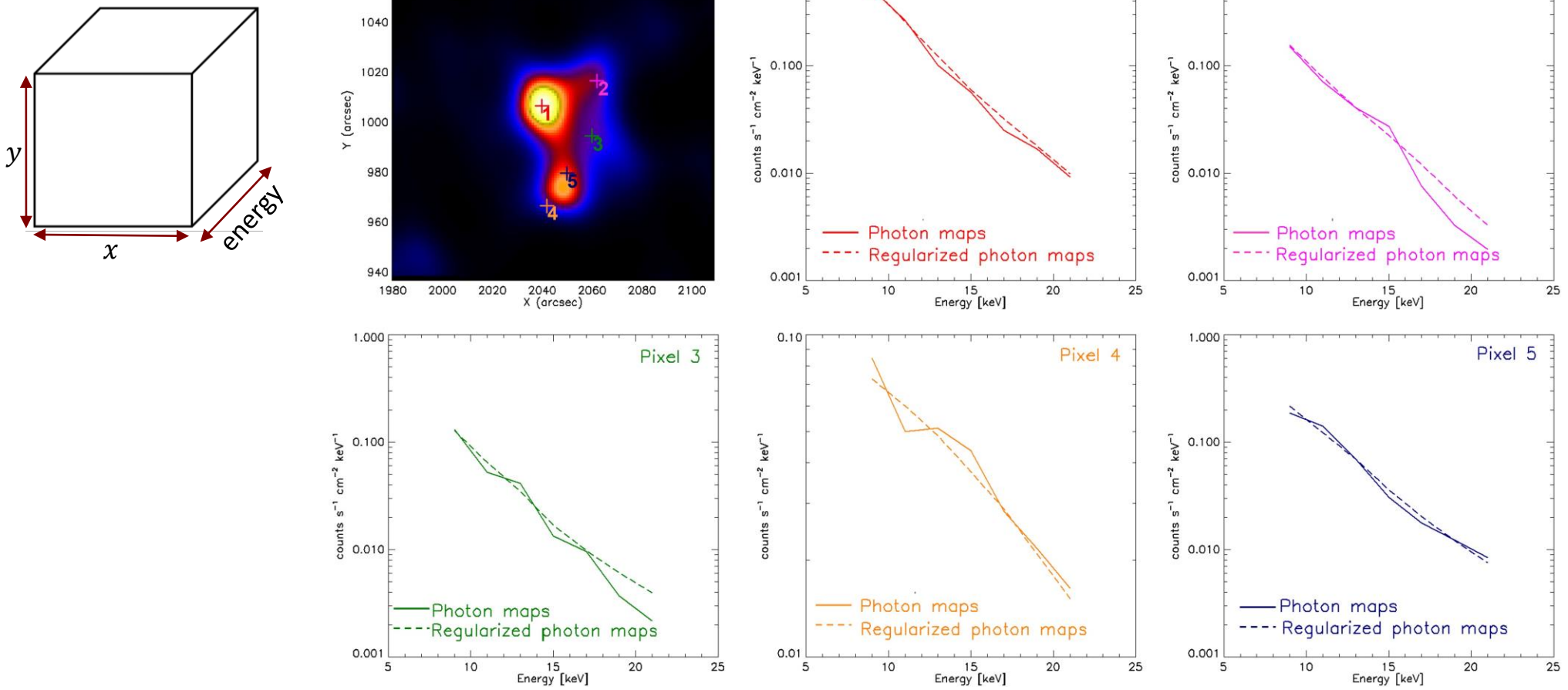

Figure: Pixel-wise spectrum obtained from photon maps and regularized photon maps. *Top left panel*: selected pixels are indicated with colored crosses. The other panels show the pixel-wise spectrum obtained from photon maps (*solid line*) and regularized photon maps (*dotted line*). The pixels selected in the top left panel and their respective spectra are indicated with the same colour. Plots are logarithmic scaled on the y-axis.

Validation

Event	OSPEX	electron maps	photon maps	regularized photon maps
May 08, 2021	$\gamma = 5.25$	$\delta = 4.53$	$\gamma = 4.94$	$\gamma = 5.50$
August 26, 2021	$\gamma = 5.47$	$\delta = 4.59$	$\gamma = 5.27$	$\gamma = 5.57$
January 20, 2022	$\gamma = 6.35$	$\delta = 4.91$	$\gamma = 6.25$	$\gamma = 6.36$
August 28, 2022	$\gamma = 6.94$	$\delta = 4.97$	$\gamma = 6.88$	$\gamma = 6.81$
September 29, 2022	$\gamma = 4.49$	$\delta = 3.68$	$\gamma = 4.24$	$\gamma = 4.42$

Table: Global spectral indices provided by OSPEX, electron maps, photon maps, and regularized photon maps.

Validation

Event	OSPEX	electron maps	photon maps	regularized photon maps
May 08, 2021	$\gamma = 5.25$	$\delta = 4.53$	$\gamma = 4.94$	$\gamma = 5.50$
August 26, 2021	$\gamma = 5.47$	$\delta = 4.59$	$\gamma = 5.27$	$\gamma = 5.57$
January 20, 2022	$\gamma = 6.35$	$\delta = 4.91$	$\gamma = 6.25$	$\gamma = 6.36$
August 28, 2022	$\gamma = 6.94$	$\delta = 4.97$	$\gamma = 6.88$	$\gamma = 6.81$
September 29, 2022	$\gamma = 4.49$	$\delta = 3.68$	$\gamma = 4.24$	$\gamma = 4.42$

Table: Global spectral indices provided by OSPEX, electron maps, photon maps, and regularized photon maps.

Validation

Event	OSPEX	electron maps	photon maps	regularized photon maps
May 08, 2021	$\gamma = 5.25$	$\delta = 4.53$	$\gamma = 4.94$	$\gamma = 5.50$
August 26, 2021	$\gamma = 5.47$	$\delta = 4.59$	$\gamma = 5.27$	$\gamma = 5.57$
January 20, 2022	$\gamma = 6.35$	$\delta = 4.91$	$\gamma = 6.25$	$\gamma = 6.36$
August 28, 2022	$\gamma = 6.94$	$\delta = 4.97$	$\gamma = 6.88$	$\gamma = 6.81$
September 29, 2022	$\gamma = 4.49$	$\delta = 3.68$	$\gamma = 4.24$	$\gamma = 4.42$

Table: Global spectral indices provided by OSPEX, electron maps, photon maps, and regularized photon maps.

STIX vs RHESSI

	STIX	**RHESSI**
Distance from the Sun	Variable	Fixed
Energy sampling	Non-uniform	Uniform
Gaps	provides its set of visibility values at all count energies → no (u, v) point gaps	gaps due to insufficient signal-to-noise as the visibility value in question → different energy bins have different number of samples

Table: Differences between STIX and RHESSI inversion software.

STIX vs RHESSI

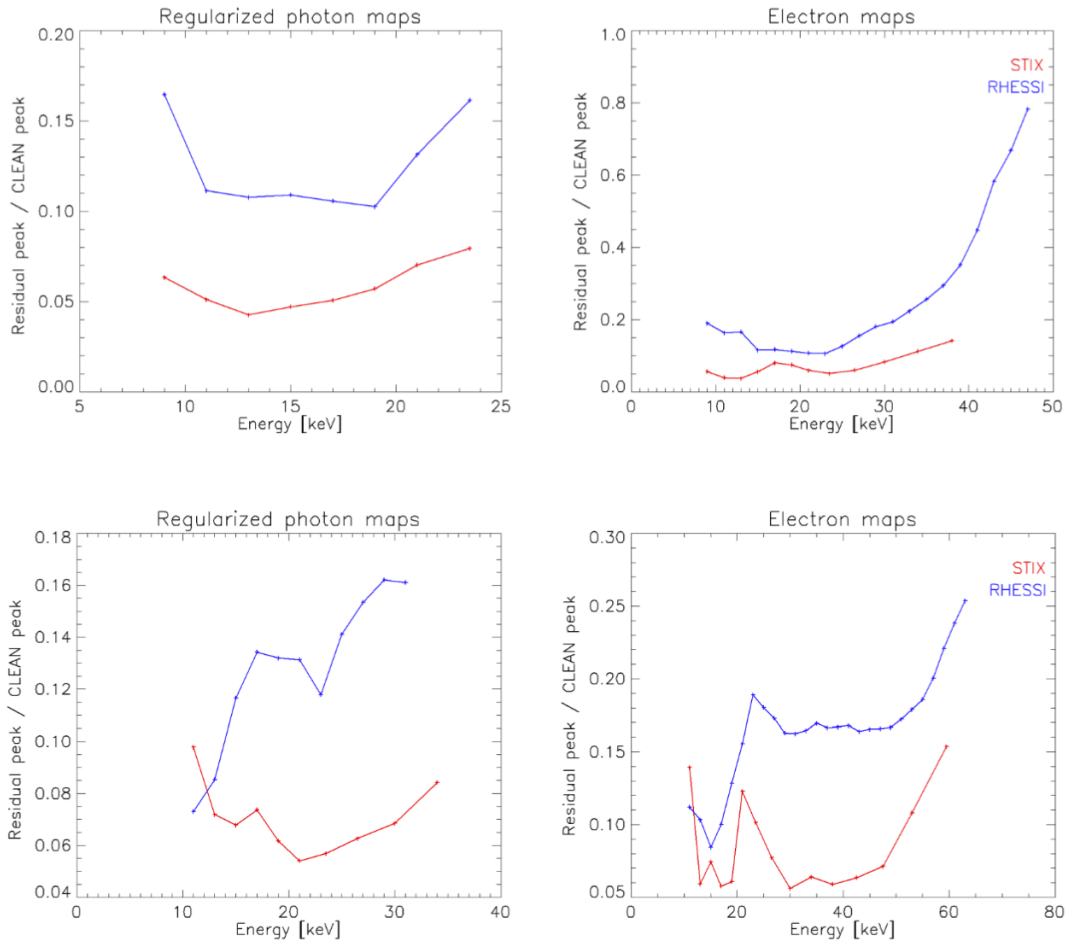

Figure: Ratio between the maximum of the residual map and the maximum of the Clean map at different energies. Red: STIX; blue: RHESSI. *Top row*: Comparison between January 11, 2023 event (STIX) and December 02, 2003 event (RHESSI). *Bottom row*: Comparison between November 11, 2022 event (STIX) and February 20, 2002 event (RHESSI)

Future works

Calibration

- ❑ Effective slit as a function of the energy;
- ❑ Apply the same strategy also for grids 1 and 2.

Imaging methods

- ❑ Test multiscale-Clean;
- ❑ Compare different methods;
- ❑ Error maps.

Electron maps

- ❑ Analize the electron transport effects to obtain:
  - the average density along the line of sight;
  - number spectrum of accelerated electrons.

THANK YOU FOR THE ATTENTION!

volpara@dima.unige.it

Università di Genova
DIMA | Dipartimento di Matematica
MIDA group

n|w

Università di Genova